

Intrinsically faint quasars: evidence for meV axion dark matter in the Universe

Anatoly A. Svidzinsky

Department of Physics, Institute for Quantum Studies, Texas A&M University, TX 77843-4242

(Dated: January 25, 2019)

Growing amount of observations indicate presence of intrinsically faint quasar subgroup (a few % of known quasars) with noncosmological quantized redshift. Here we find an analytical solution of Einstein equations describing bubbles made from axions with periodic interaction potential. Such particles are currently considered as one of the leading dark matter candidate. The bubble interior possesses equal gravitational redshift which can have any value between zero and infinity. Quantum pressure supports the bubble against collapse and yields states stable on the scale more than hundreds million years. Our results explain the observed quantization of quasar redshift and suggest that intrinsically faint point-like quasars associated with nearby galaxies are axionic bubbles with masses 10^8 - $10^9 M_\odot$ and radii 10^3 - $10^4 R_\odot$. They are born in active galaxies and ejected into surrounding space. Properties of such quasars unambiguously indicate presence of axion dark matter in the Universe and yield the axion mass $m \approx 1$ meV, which fits in the open axion mass window constrained by astrophysical and cosmological arguments.

Based on observations, Karlsson [1] has noted division of quasars (QSOs) into two groups with different redshift properties and concluded the following. If we select QSOs associated with most nearby (distance $d \lesssim 50$ - 100 Mpc), galaxies then their redshift is close to certain values (quantized), as shown in Fig. 3 below. Meanwhile, in QSO samples associated with distant galaxies no periodicity in intrinsic redshift is observed. Such a division is supported by later studies of QSOs associated with most nearby galaxies where the quantization was confirmed [2, 3] and distant ($0.01 < z_{\text{gal}} < 0.3$) galaxies for which absence of any periodicity was claimed [4]. The observations suggest existence of intrinsically faint (optical luminosity $L = 10^5$ - $10^7 L_\odot$) QSO subgroup with quantized noncosmological redshift. Being intrinsically faint, such objects are not detected from large distances (which yields disappearance of redshift quantization in distant QSO samples) and constitute only a few % of the known QSO population. Observations indicate that such quasars are ejected from nearby active galaxies or in the process of ejection from the galactic nucleus [5, 6].

Here we show that bubbles of dark matter with periodic interaction potential, masses about 10^8 - $10^9 M_\odot$ and radii 10^3 - $10^4 R_\odot$ can explain the intrinsically faint quasars. The bubble is supported against collapse by quantum pressure and decays on a time scale more than hundreds million years. Hypothetical axions, one of the leading dark matter candidate, fit well into this picture and can account for the redshift quantization. Usual baryonic matter falls into the bubble interior, heated by the release of the gravitational energy and produce electromagnetic radiation that freely propagate into surrounding space.

In this Letter we study massive real scalar field φ with periodic interaction potential

$$V(\varphi) = V_0[1 - \cos(\varphi/f)], \quad (1)$$

where $V_0 > 0$. This potential is quite general and derived in quantum field theory in connection with pseudo Nambu-Goldstone bosons (PNGBs) [7]. In all such mod-

els, the key ingredients are the scales of global symmetry breaking f and explicit symmetry breaking $(V_0)^{1/4}$. One of the examples of a light hypothetical PNGB is the axion which possess extraordinarily feeble couplings to matter and radiation and is well-motivated dark matter candidate [8]. If the axion exists, astrophysical and cosmological arguments constrain its mass to be in the range of $m = 10^{-6} - 3 \times 10^{-3}$ eV and the global symmetry-breaking scale to lie in a window $f \approx 10^7$ GeV $\times 0.62/m(\text{eV}) = 2 \times 10^9 - 6 \times 10^{12}$ GeV [8].

We consider spherically symmetric system with metric

$$ds^2 = -N^2 dt^2 + g^2 dr^2 + r^2 d\Omega^2, \quad (2)$$

where g , the radial metric, and N , the lapse, are functions of t and r with r being the circumferential radius. We introduce dimensionless coordinates and define the unit of distance, time and φ as

$$r_0 = \frac{\hbar}{mc}, \quad t_0 = \frac{\hbar}{mc^2}, \quad \varphi_0 = \frac{1}{\sqrt{4\pi G}}, \quad (3)$$

where c is the speed of light, G is the gravitational constant, $m = \sqrt{V_0}/f$ is the particle mass. In dimensionless units the static Klein-Gordon and Einstein equations describing the self-gravitating field φ and the metric are [9]

$$\frac{\varphi'}{g^2} \left(\frac{g^2 + 1}{r} - 2rg^2V \right) + \frac{\varphi''}{g^2} - \frac{\partial V}{\partial \varphi} = 0, \quad (4)$$

$$N' = \frac{N}{2} \left[\frac{g^2 - 1}{r} + r(\varphi'^2 - 2g^2V) \right], \quad (5)$$

$$g' = \frac{g}{2} \left[\frac{1 - g^2}{r} + r(\varphi'^2 + 2g^2V) \right], \quad (6)$$

with boundary conditions

$$g(0) = g(\infty) = N(\infty) = 1,$$

$$g'(0) = N'(0) = \varphi'(0) = 0, \quad V(\varphi(\infty)) = 0,$$

where prime denotes $\partial/\partial r$,

$$V = \frac{1}{\alpha^2} [1 - \cos(\alpha\varphi)], \quad \alpha = \frac{1}{\sqrt{4\pi G f}} = \frac{m_{\text{pl}}}{\sqrt{4\pi f}} \quad (7)$$

is the dimensionless potential and the coupling parameter respectively, $m_{\text{pl}} = \sqrt{\hbar c/G} = 1.2 \times 10^{19}$ GeV is the Planck mass. The interaction potential has degenerate minima at $\varphi = 2\pi n/\alpha$, where n is an integer number. Here we show that in the limit of strong nonlinearity, $\alpha \gg 1$, Eqs. (4)-(6) have an approximate static solution that describes a spherical bubble with surface width much smaller than its radius R . The bubble surface is an interface between two degenerate vacuum states with $\varphi = 2\pi n/\alpha$ ($r < R$) and $\varphi = 0$ ($r > R$).

Outside the bubble Eqs. (4)-(6) lead to the known Schwazschild solution

$$g^2 = \frac{1}{1 - 2M/r}, \quad N^2 = 1 - \frac{2M}{r}, \quad (8)$$

where M is the bubble mass in units of m_{pl}^2/m .

Let us assume that $R \gg \alpha \gg 1$. Then, near the surface one can omit terms with $1/r$ in Eqs. (4)-(6) and take $r \approx R$, we obtain

$$-2R\varphi'V + \frac{\varphi''}{g^2} - \frac{\partial V}{\partial \varphi} = 0, \quad (9)$$

$$N' = \frac{NR}{2} (\varphi'^2 - 2g^2V), \quad (10)$$

$$g' = \frac{gR}{2} (\varphi'^2 + 2g^2V). \quad (11)$$

Eqs. (9)-(11) can be solved analytically. Their first integral is

$$N = \text{const}, \quad \varphi'^2 = 2g^2V, \quad g' = Rg\varphi'^2. \quad (12)$$

We assume $\varphi(0) = 2\pi n/\alpha$, where $n = 1, 2, 3, \dots$ is the number of kinks at the bubble surface, and $\varphi(r)$ monotonically decreases with r . Eqs. (12) yield

$$\frac{1}{g} = 1 - R \int_{\varphi}^{\varphi(0)} \sqrt{2V} d\varphi, \quad \varphi' = -\frac{\sqrt{2V}}{1 - R \int_{\varphi}^{\varphi(0)} \sqrt{2V} d\varphi}. \quad (13)$$

For $V(\varphi)$ given by Eq. (7) the final solution is

$$\frac{4R}{\alpha^2} \ln |\sin(\alpha\varphi/2)| + \left[1 - \frac{4R}{\alpha^2} (2m - 1) \right] \text{arctanh}[\cos(\alpha\varphi/2)]$$

$$= \text{sign}[\sin(\alpha\varphi/2)](r - R_m),$$

$$\varphi \in [2\pi(n - m + 1)/\alpha, 2\pi(n - m)/\alpha], \quad (14)$$

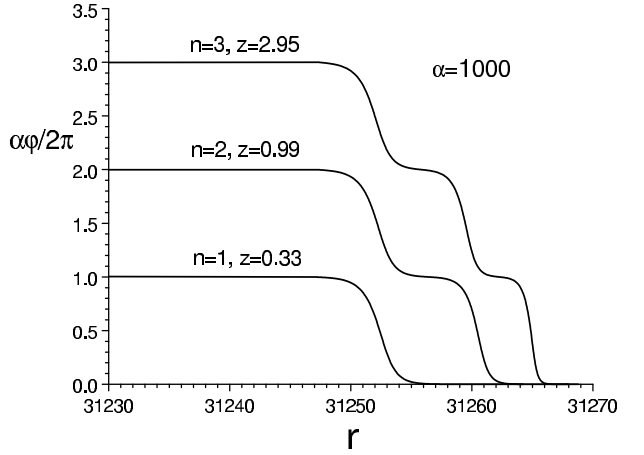


FIG. 1: Scalar field φ as a function of distance r to the bubble center for bubbles with equal radius and different quantum numbers $n = 1, 2, 3$. The unit of length is \hbar/mc . Note, we plot the field φ only in the vicinity of the bubble surface where it undergoes variation.

where R_m is a position of the m th kink, $m = 1, 2, \dots, n$. When the coordinate r passes through the point R_m the scalar field $\varphi(r)$ changes from $2\pi(n - m + 1)/\alpha$ to $2\pi(n - m)/\alpha$ (see Fig. 1). Eq. (13) yields the following expression for g as a function of φ inside the bubble:

$$\frac{1}{g} = 1 - \frac{4R}{\alpha^2} [2m - 1 + \cos(\alpha\varphi/2)]. \quad (15)$$

Outside the bubble $\varphi = 0$, $m = n$ and $1/g = 1 - 8nR/\alpha^2$. The solution is valid if $1/g > 0$, that is $R < R_{\text{max}} = \alpha^2/8n$. Match of the inner solution (13) with the Schwazschild solution (8) determines the mass-radius relation

$$M = 4\pi n u R^2 - 8\pi^2 n^2 u^2 R^3, \quad (16)$$

where u is the surface energy density given by an integral over one potential period $u = \int \sqrt{2V} d\varphi/4\pi$. For the cosine potential (7) $u = 2/\pi\alpha^2$.

Redshift of the bubble interior $z = 1/N - 1$ can be found by matching the inner $N = \text{const}$ and the outer (8) solutions:

$$z = \frac{1}{\sqrt{1 - 2M/R}} - 1 = \frac{1}{1 - 4\pi n u R} - 1. \quad (17)$$

The internal redshift monotonically increases from zero to infinity when the bubble radius R changes from zero to R_{max} . Fig. 2 shows the redshift of space as a function of the distance r to the bubble center. The redshift is constant in the bubble interior and monotonically decreases outside the bubble.

Let us make rescaling $M \rightarrow M/4\pi u$, $R \rightarrow R/4\pi u$, then Eqs. (16), (17) yield

$$M = nR^2 - n^2R^3/2, \quad z = \frac{1}{1 - nR} - 1. \quad (18)$$

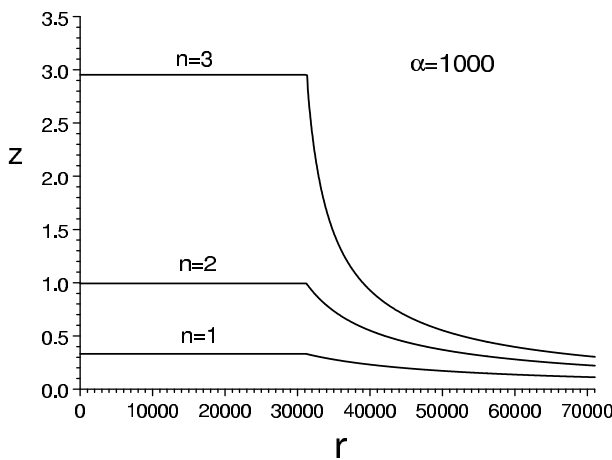


FIG. 2: Redshift z of space as a function of distance r to the bubble center for bubbles shown in Fig. 1.

For a given M the redshift depends on the integer number n , which implies the redshift is quantized.

In early samples of QSOs associated with nearby spiral galaxies, Karlsson showed that the redshift distribution has a periodicity $\log(1 + z_{n+1}) - \log(1 + z_n) = 0.089$, where $n = 0, 1, 2, \dots$ and $z_0 = 0.061$ [10]. It has been later confirmed by other groups [2, 11]. In a recent paper, Burbidge and Napier [3] tested for the occurrence of this periodicity in new QSO samples and found it to be present at a high confidence level. The peaks were found at $z \approx 0.30, 0.60, 0.96, 1.41$ and 1.96 in agreement with Karlsson's empirical formula. The formula also includes the peak at $z_0 = 0.061$, however, this peak does not occur for quasars, but for morphologically related objects.

The redshift periodicity is observed only in QSO samples satisfying certain selection criteria, in particular, the galaxies which are assumed to be paired to the QSOs must be *most nearby* spirals [1, 12]. This implies that redshift quantization is a property of intrinsically faint QSOs which are not detected from large distances.

It is naturally to assume that QSOs born in the same type of galaxies have approximately equal masses because their formation mechanism must be similar. Such phenomenon is well known for type Ia supernovae or neutron stars: practically all measured neutron star masses cluster around the value of $1.4M_{\odot}$ with only a few percent deviation [13]. If dark matter bubbles are born with equal masses then, according to Eqs. (18), their redshift must be quantized. For $M = 0.0601$ (in dimension units $M = 0.00752\alpha^2 m_{\text{pl}}^2/m$) Eqs. (18) have solutions for $n = 1, 2, \dots, 8$, they are given in Table 1.

In Fig. 3 we plot the most recent histogram of the redshift distribution from Ref. [12] in which five peaks are clearly seen. The solid lines show the redshifts from our Table 1, they match well the observed peaks. The agreement is remarkable because the theory has only one free parameter, the bubble mass M . Such coincidence strongly suggests that the point-like quasars associated

n	R, in $\alpha^2 \hbar/mc$	z
1	0.0329	0.357
2	0.0241	0.629
3	0.0204	0.96
4	0.0182	1.40
5	0.0168	2.06
6	0.0159	3.24
7	0.0153	6.11
8	0.0151	26.6

TABLE I: Redshift of the bubble interior z and its radius R for $M = 0.00752\alpha^2 m_{\text{pl}}^2/m$ and different kink numbers n .

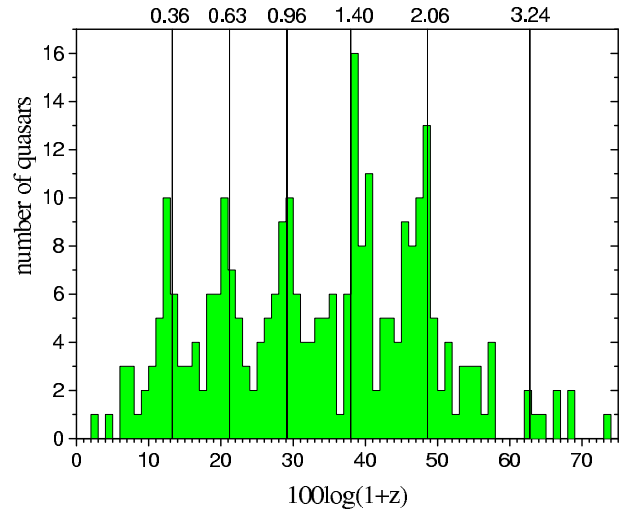


FIG. 3: Histogram of the redshift distribution of QSOs close to bright nearby active spiral galaxies or multiple QSOs with small angular separation from Ref. [12]. The solid lines represent position of the peaks from Table 1.

with nearby galaxies are dark matter bubbles composed of scalar particles with periodic interaction potential. One should mention an alternative possibility of quasar evolution. Bubbles can be originally born with the same mass and number of kinks $n = 5$ that corresponds to the 5th peak. During evolution the kinks tunnel to the bubble center and quasars sequentially decay into states with smaller n but the same mass.

For axions with $m = 0.1 - 3$ meV and $f = 2 \times 10^9 - 6 \times 10^{10}$ GeV Eq. (7) yields $\alpha = 5.6 \times 10^7 - 1.7 \times 10^9$. Hence, an axion bubble with the internal redshift $z = 0.36$ and $n = 1$ would have the mass $M = 3 \times 10^7 - 10^9 M_{\odot}$ and the radius $R = 3 \times 10^2 - 10^4 R_{\odot}$. Such radius range agrees with the size of the emission region expected for the intrinsically faint QSOs. Indeed, for Seyfert 1 galaxies the size of the broad-line region is $R \sim 10 - 100$ light days. The luminosity L of the QSOs is 5-6 orders smaller. Based on the empirical relation for Seyfert 1 galaxies $R \propto L^{1/2}$ [14], we obtain for the quasars $R \sim 10^4 R_{\odot}$.

Now we discuss the bubble life time. Under the influence of surface tension and gravitational attraction an initially static bubble starts to collapse. In the thin-wall approximation the initial acceleration is given by [15]

$$\ddot{R} = -\frac{2N^3}{R} - \frac{N^2 M}{(1+N)R^2}, \quad (19)$$

where $N = \sqrt{1-2M/R}$. For one kink thin-wall contracting bubble the conserved mass is [15]

$$M = \frac{4\pi u R^2}{\sqrt{1 - (dR/d\tau)^2}} - 8\pi^2 u^2 R^3, \quad (20)$$

where τ is the interior coordinate time. Based on Eqs. (19), (20) one can expect a continuous contraction of the bubble to the origin on an astronomically short time scale $R/c \ll 1\text{yr}$. However, so far we treated the scalar field as classical. Quantum corrections suppress the collapse and result in appearance of long-lived bubbles, stable on a scale more than hundreds million years. To include quantum effects it has been suggested that the expression (20) be interpreted as the canonical hamiltonian of the bubble at the quantum level [16, 17, 18]. The bubble wave function $\Psi(R)$ satisfies the following stationary quantum mechanical equation in one dimension ($\hbar = 1$) [18]:

$$\left[(E + 8\pi^2 u^2 R^3)^2 + \frac{\partial^2}{\partial R^2} - 16\pi^2 u^2 R^4 \right] \Psi(R) = 0. \quad (21)$$

This equation possesses stationary solutions that are not possible in the classical model. Bubbles of non-negligible redshift correspond to highly excited stationary states for which the energy spectrum can be treated as quasi-continuous. At the quantum level the collapse is prevented by quantum pressure that balances the surface tension and gravitational attraction producing stationary configurations.

Let us estimate the decay time of an excited stationary state of the quantum bubble. The decay occurs by means of scalar particle emission. We estimate the decay time using the Bohr correspondence principle as the time of energy loss by the classical bubble with the radius $R(t)$ oscillating between the turning points $R(t) = R$ and $R(t) = 0$, where R is determined by Eq. (16). In the quantum picture, however, there are no such oscillations. The probability of creation a particle with the

energy mc^2 by a moving bubble surface is governed by the Boltzmann factor $\exp(-mc^2/T_{\text{eff}})$, where $T_{\text{eff}} = a/c$ is the effective temperature and a is the acceleration of the surface [19]. For the bubble $a \approx c^2/R(t)$ and the Boltzmann factor reduces to $\exp(-R(t)/l)$ where $l = \hbar/mc$ is the surface width. Hence, emission of scalar particles is exponentially suppressed apart from small regions where $R(t) \lesssim l$. As a result, during one period of oscillation, $t_c \sim R/c$, the energy loss is $\Delta E \sim (l/R)E$, which yields the bubble life time

$$t \sim \frac{R}{l} t_c = \frac{R^2}{cl}. \quad (22)$$

For an axionic bubble with $R > 10^2 R_\odot$ and $l < 0.7 \text{ cm}$ Eq. (22) yields $t > 10^8 \text{ yrs}$ which is the time we need to account for the phenomenon of quasars.

Properties of the intrinsically faint point-like QSOs, combined with equations for the bubble mass $M = 0.00752\alpha^2 m_{\text{pl}}^2/m = 2.94m(\text{eV}) \times 10^{11} M_\odot$ and the radius $R = 0.0329\alpha^2 \hbar/mc = 2.73m(\text{eV}) \times 10^6 R_\odot$, allow us to determine the axion mass m . The quasar luminosity suggests that the bubble radius is larger then $10^3 R_\odot$ which yields $m > 0.4 \text{ meV}$ and $M > 10^8 M_\odot$. From the other hand, the quasar ejection from active galaxies implies that the bubble mass M must be much smaller then the galactic mass. It is reasonable to constrain $M < 10^9 M_\odot$ which leads to $m < 3 \text{ meV}$ and $R < 10^4 R_\odot$. We conclude, the axion mass is $m = 0.4 - 3 \text{ meV}$. This value fits in the open window for the axion mass constrained by astrophysical and cosmological arguments [8], which unambiguously points towards the axionic nature of dark matter composing the intrinsically faint point-like quasars. Current cavity search experiments in Livermore [20] and Kyoto University [8] are looking for the axion in the mass range $1 - 10 \mu\text{eV}$ which deviates by two orders of magnitude from our result. Probably now, when the axion mass is established from quasar observations, the axion has a better chance to be discovered.

We mention that data on central “black hole” masses in small companion galaxies allow us to determine the axion mass more accurately and yield $m = 1.0 - 1.9 \text{ meV}$. We will discuss this elsewhere. Moreover, observations show that apart from the intrinsically faint point-like objects considered here there is a subgroup of bright quasars which probably also possess noncosmological redshift. Tachyons, another dark matter candidate, can explain their nature. We discuss this in a detail paper [21].

[1] K.G. Karlsson, A&A **239**, 50 (1990).
[2] H. Arp *et al.*, A&A **239**, 33 (1990).
[3] G. Burbidge and W.M. Napier, AJ **121**, 21 (2001).
[4] E. Hawkins, S.J. Maddox and M.R. Merrifield, MNRAS **336**, L13 (2002).
[5] G.R. Burbidge *et al.*, ApJS **74**, 675 (1990); E.M. Burbidge *et al.*, ApJ **591**, 690 (2003); H. Arp *et al.*, A&A **391**, 833 (2002); A&A **418**, 877 (2004).
[6] H. Arp, *Quasars, redshifts and controversies*, Interstellar Media, Berkeley, 1987; *Seeing red: redshifts, cosmology and academic science*, Apeiron, Montreal, 1998.
[7] C.T. Hill and G.G. Ross, Nucl. Phys. B**311**, 253 (1988).
[8] R. Bradley *et al.*, Rev. Mod. Phys. **75**, 777 (2003).
[9] E. Seidel and W. M. Suen, Phys. Rev. D **42**, 384 (1990).

- [10] K.G. Karlsson, A&A **13**, 333 (1971); **58**, 237 (1977).
- [11] J.M. Barnothy and M.F. Barnothy, PASP **88**, 837 (1976).
- [12] W.M. Napier and G. Burbidge, MNRAS **342**, 601 (2003).
- [13] N.K. Glendenning, “Compact Stars: Nuclear Physics, Particle Physics, and General Relativity”, Springer Verlag; New York, 2nd edition, (2000).
- [14] T.G. Wang and X.G. Zhang, MNRAS **340**, 793 (2003).
- [15] S. K. Blau *et al.*, Phys. Rev. D **35**, 1747 (1987).
- [16] V.A. Berezin *et al.*, Phys. Lett. B **212**, 415 (1988).
- [17] A. Aurilia and E. Spallucci, Phys. Lett. B **251**, 39 (1990).
- [18] A. Aurilia *et al.*, Phys. Lett. B **262**, 222 (1991).
- [19] A. Gorsky and K. Selivanov, Phys. Rev. D **62**, 071702 (2000).
- [20] S.J. Asztalos *et al.*, Phys. Rev. D **69**, 011101(R) (2004).
- [21] A.A. Svidzinsky, astro-ph/0409064.